

Trans. Nonferrous Met. Soc. China 19(2009) s343-s348

Transactions of Nonferrous Metals Society of China

www.tnmsc.cn

Microstructural evolution of spray-formed Al-11.5Zn-2.0Mg-1.6Cu alloy during hot-extrusion and heat-treatment

GUO Shu(郭 舒), NING Zhi-liang(宁志良), CAO Fu-yang(曹福洋), SUN Jian-fei(孙剑飞)
School of Materials Science and Engineering, Harbin Institute of Technology, Harbin 150001, China
Received 10 June 2009; accepted 15 August 2009

Abstract: Al-11.5Zn-2.0Mg-1.6Cu alloy was synthesized by spray forming (SF) technique followed by hot extrusion and heat-treatment. Its microstructural evolution was investigated by scanning electron microscopy (SEM), transmission electron microscopy (TEM) with energy dispersive spectroscopy (EDS) and X-ray diffraction (XRD) in the whole process. The curve of hardness as a function of aging time was obtained at 120 . Test results indicate that the grain morphology is equiaxed and uniform in the central region of the spray-formed billet, but fine and irregular in the bottom and top regions. Both the grain boundary and the intragranular phases are identified as $MgZn_2$ intermetallics. Hot extrusion promotes the refinement of the microstructure. Grain boundary phase disappears, meanwhile, η -phase (MgZn₂) and Al₃Zr particles precipitate from the matrix after extrusion. The alloy reaches its maximum hardness after being aged at 120 for 14 h, associated with a massive precipitation of intermediate η' -phase (MgZn) in the matrix.

Key words: Al-Zn-Mg-Cu alloy; spray forming; microstructure; hot extrusion; aging

1 Introduction

Al-Zn-Mg-Cu alloys, series commercially trademarked as $7 \times \times \times$ Al-alloys, have well-known applications in the field of aircraft industry for their high levels of strength, high fracture toughness and relatively low densities[1]. For this series of alloys, the precipitation-hardening arising from the structural particles, such as GP zones, $\eta'(MgZn)$ and $\eta(MgZn_2)$, formed at aging stage after solid solution treatment plays a key role in the improvement of their strength performance[2-3]. Thus, it is an effective method to improve their mechanical properties by increasing the numbers of precipitated particles in the matrix of the alloys. Many investigations[2-4] have shown that the aging properties of 7××× Al alloys can be obviously improved by increasing the zinc content, due to the fact that it enhances the extent of solute supersaturation, then promotes precipitation-hardening. However, if the mass fraction of zinc is over 8%, low cooling rate of ingot metallurgy (IM) process results in several serious foundry defects, such as cracking, macro-segregation and coarse microstructure in these alloys. So, high solute alloys can be produced only through rapid solidification

processes[5].

In the last decade, more interest focused on using spray forming (SF) technique to improve the strength level of $7\times\times\times$ Al alloys. SF technique, which was firstly introduced by Singer and developed by Osprey Metals Ltd., combines melt atomization and deposition into one single-step process[6]. It shows great advantages in many aspects, for instance, eliminating macro-segregation, promoting the formation of refined grains and extending the solubility of alloy elements[6–8]. Thereby, it is much suitable for the preparation of high solute Al-Zn-Mg-Cu series alloys.

In the present study, a new Al-Zn-Mg-Cu alloy with zinc of 11.5% (mass fraction) was synthesized using the SF process, followed by hot extrusion and heat treatment to obtain end-product performance. The main work was done on characterization of its microstructural evolution in the process. The variation of aging hardness with one-step aging time was also investigated.

2 Experimental

The master alloy with nominal composition of 11.5% Zn, 2.0% Mg, 1.6% Cu, 0.2% Zr and balance Al was prepared from industrial grade materials. The SF

experiment was carried out on a vacuum SF equipment with a close-type atomization nozzle. A rotating deposition substrate was placed under the nozzle. The main parameters used in the experiment are listed in Table 1. During the experiment, the substrate was continuously moved in the opposite direction of billet growing to enable the atomized droplets to fly over a constant distance. The as-deposited billet was machined off to 100 mm in diameter, and subsequently hotinto round rods at an extrusion extruded at (400 ± 10) ratio of 28:1. The purposes of hot deformation are to eliminate the porosity in deposition and refine grains and the second phases. The extruded rods were treated in salt bath at 480 for 1.5 h, then immediately quenched in water to room temperature. The one-step temper process was chosen which involved aging at 120 for up to 80 h.

Table 1 Primary spay forming parameters

Parameter	Condition		
Backfill gas	Nitrogen		
Atomization gas	Nitrogen		
Atomization pressure/MPa	2.0		
Pour temperature/	780-800		
Deposition distance/mm	400		

The microstructures were characterized using a Quanta 200 model scanning electron microscope (SEM) and a Philips CM12 model transmission electron microscope (TEM). The SEM specimens were etched using Keller reagent, and the TEM discs were mechanically ground down to 50 μ m, then twin-jet polished with a 10% nitric acid + 80% methanol solution at -20 . X-ray diffraction (XRD) studies were done on a Japan Rigaku diffractometer with Cu K $_{\alpha}$ radiation. Vickers hardness was measured after being aged for different time.

3 Results and discussion

3.1 Characterization of as-deposited microstructures

The as-deposited microstructures at different sections of SFed Al-11.5Zn-2.0Mg-1.6Cu alloy billet is shown in Fig.1. Fig.1(a) shows the microstructure in 1–2 mm away from the substrate, formed at the initial stage of SF process, which consists of the fine spherical grains. The grains are not uniform in size in this region, and some of them are more than 20 µm or less than 5 µm in diameter. Moreover, several grains look pre-solidified powders and traces of irregular deformation are observed in some areas. Similar results are also reported in Ref.[9]. The microstructure in the central region of the billet is typically shown in Fig.1(b). The equiaxed grains in this region have an average size

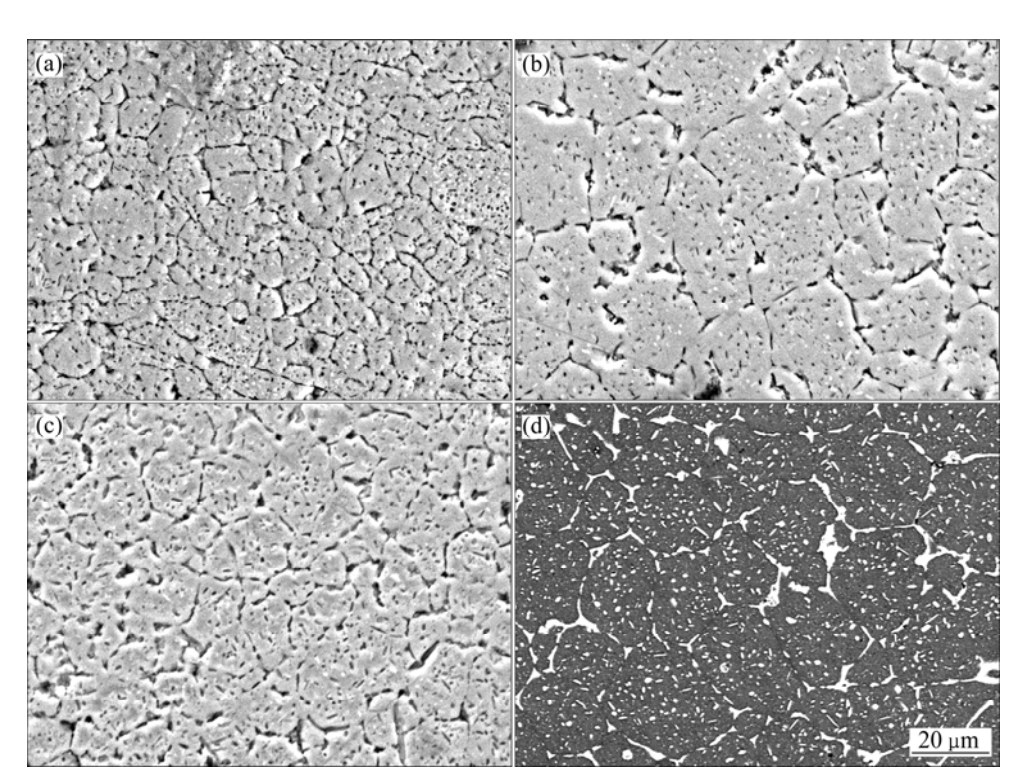


Fig.1 SEM micrographs of as-deposited Al-11.5Zn-2.0Mg-1.6Cu alloy at different sections: (a) Bottom; (b) Center; (c) Top; (d) BSE image of central region

of about 25 μ m in diameter, being obviously bigger and more uniform than those shown in Fig.1(a).

As reported by many investigators[8-10], atomized droplets, most of which keep partially solidified during the flight course, gradually accumulate and form a semi-liquid layer on top of the billet containing a large number of broken dendrite fragments. These dendrite fragments act as heterogeneous nucleus. temperature decreases, the nucleus homogeneously grow and finally meet each other at the interface, leading to the morphology of spherical grains as shown in Fig.1(b). However, at the initial stage of SF, partial and full liquid atomized droplets will directly impinge on the substrate before the formation of semi-liquid layer, rapidly spread out and solidify to form a lamellar structure. While some full solid-state droplets are embedded in the deposited billet retaining their original microstructures. In a word, chilling action of the substrate as well as lack of liquid state make the grains at the bottom fine and irregular corresponding to the alloy shown in Fig.1(a). Fig.1(c) illustrates the microstructure in the top region of the deposited billet, where the grain morphology is similar to that in the central region, but differs in the size distribution. Exposed to the atomization atmosphere, this region has a higher heat extraction rate. Thus, microstructure is relatively fine in size as a result of inhibition of grains coarsening and coalescence.

Fig.1(d) shows the back scattered electron (BSE) image revealing the morphology and the distribution of secondary phases in the as-deposited Al-11.5Zn-2.0Mg-1.6Cu alloy. It is apparent that two types of secondary phases are generated. One that has particle-like profile is uniformly dispersed inside $\alpha(Al)$ grains, while the other is discontinuously located at the interface. Both of them give rise to brighter contrast than $\alpha(Al)$ matrix, which suggests they contain higher content of Zn or Cu elements. By means of XRD analysis in Fig.2, a HCP MgZn₂ compound is determined. Figs.3(a) and (b) show the TEM micrographs of the intragranular and the boundary phases in the alloys, respectively. The calculated data (shown in Table 2) from selected area electron diffraction (SAED) patterns are both consistent with the lattice parameters of MgZn₂. In addition, energy dispersive spectroscopy (EDS) indicates that there are considerable amounts of Al and Cu elements in them. As no more than 1% Al can be dissolved in η -phase (MgZn₂)[11], signal detected by EDS is probably from the matrix. Whereas Cu element definitely exits in the η phase, because the matrix dissolves Cu less than 1% (molar fraction).

MONPAL et al[12] pointed out that η phase was one of the dominant secondary phases (the other is Al₂Mg₃Zn₃ phase) in the microstructures of as-cast Al-Zn-Mg-Cu alloys, which usually comes from non-

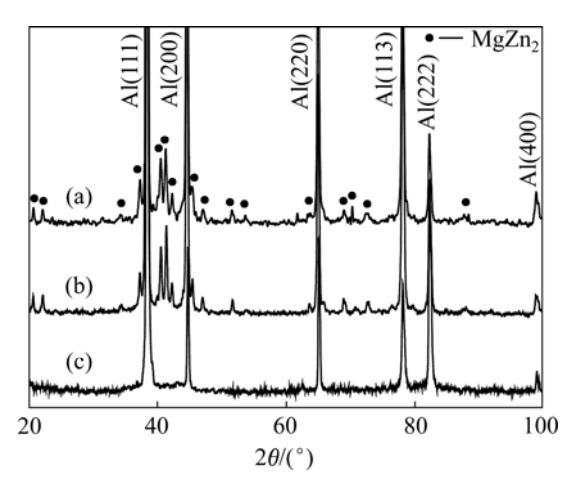


Fig.2 X-ray diffraction patterns of Al-11.5Zn-2.0Mg-1.6Cu alloy: (a) As-deposited; (b) As-extruded; (c) As-solutionized

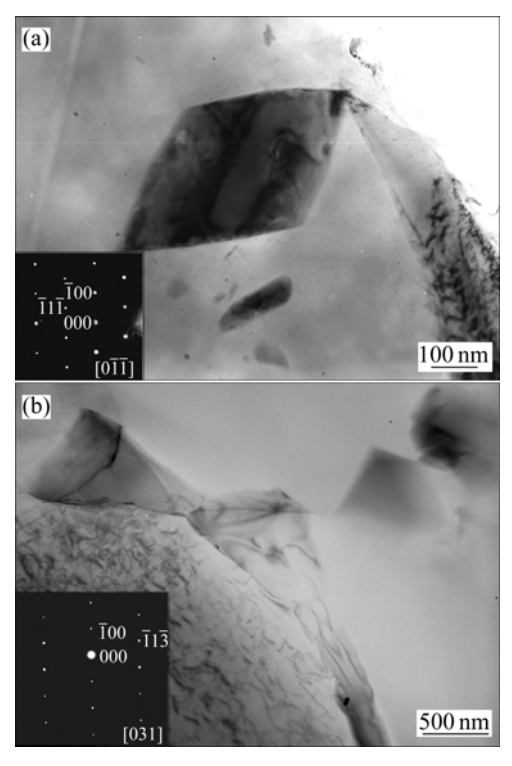


Fig.3 TEM micrographs with SAED patterns showing intragranular(a) and boundary(b) phases of as-deposited Al-11.5Zn-2.0Mg-1.6Cu alloy

equilibrium eutectic. In their research on as-cast 7055 alloys, $T(Al_2Mg_3Zn_3)$, $S(Al_2CuMg)$ and $\theta(Al_2Cu)$ phases were determined except η -phase. And Ref.[13] also reported the SFed Al-10.8Zn-2.8Mg-1.9Cu alloy contained CuMgZn, η and θ phases. But no other phases were found in the present work, and this is possibly attributed to the high mass ratio of Zn to Mg and the low copper content of the Al-11.5Zn-2.0Mg-1.6Cu alloy. That is, high mass ratio of Zn to Mg of alloy close to that of MgZn₂ compound leads to the formation of a single secondary phase during solidification, and small amount

Position of phase —	Lattice parameters		Molar fraction/%			
	a/nm	c/nm	Mg	Zn	Al	Cu
Interior	0.520	0.851	28.71	30.58	34.64	6.07
Boundary	0.516	0.843	26.07	30.73	36.48	6.72

Table 2 Lattice parameters and EDS results of η -phase (MgZn₂) in as-deposited alloy

of Cu is preferentially dissolved into the matrix and MgZn₂ phases rather than forming S and θ phases with other elements.

3.2 Microstructural evolution during extrusion process

The as-deposited alloy was hot-extruded to full density. Phase identification after extrusion was done by XRD as shown in Fig.2. It is clearly seen that η -phase is still the dominant precipitate in the as-extruded alloy. No additional new phase is evidently detected in the XRD result. Fig.4 shows the TEM images of the grains and precipitates' of the as-extruded alloy. The elongated grains are observed in Fig.4(a), with a remarkable decrease in size compared to that of the as-deposited alloy. The presence of high density intragranular dislocations and subgrains suggest that no obvious recrystallization occurs after the deformation. The large-size phases, both on boundaries and within grains, disappear in the as-extruded microstructure, instead, a large number of nanometer or submicron-size phases

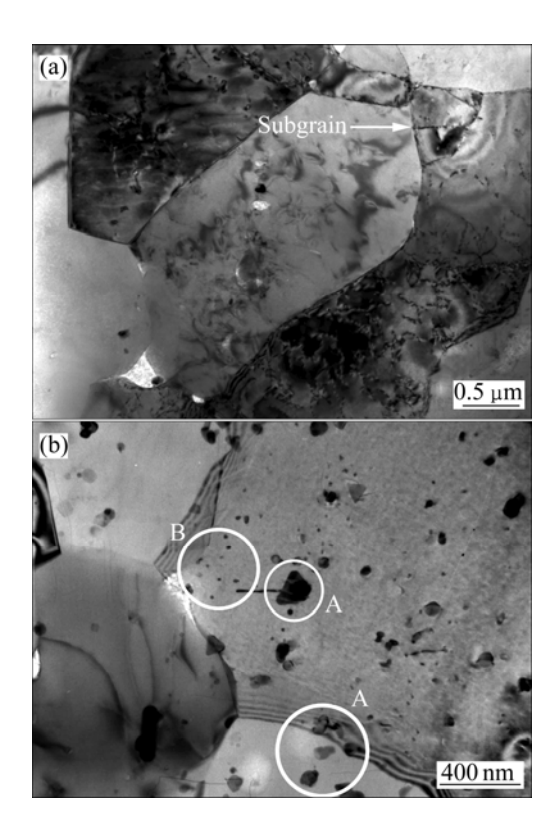


Fig.4 TEM micrographs showing grain structure(a) and intragranular phase(b) of as-extruded Al-11.5Zn- 2.0Mg-1.6Cu alloy

precipitate. It can be seen from Fig.4(b) that there are two different particles, denoted as A and B, in the grains interior. Particle A is identified as η -phase(MgZn₂), which has irregular shape and approximate 100–200 nm in diameter. Fine spherical precipitate B is Al₃Zr intermetallic according to EDS results and other descriptions[14–15]. Al₃Zr phase is likely to be generated in the process of hot-extrusion since it is not observed in the as-deposited microstructure.

In Refs.[4, 16], hot plastic deformation for as-deposited materials aims at the elimination of porous defects generated in depositing process. In fact, hot deformation plays another two important roles. Firstly, it replaces the homogenizing treatment procedure in as-cast alloys. In general, it is necessary for as-cast $7 \times \times \times$ alloys to homogenize the grain-boundary segregation through a long-time diffusion annealing. However, secondary phases in spray-formed materials are so small in size that a preheated treatment before deformation process can even make the microstructure more uniform. Secondly, hot deformation leads to a microstructural refinement and a solid-state phase transformation. It can be seen from the TEM results that grain-size decreases as a result of not only fragmentation of large grains but also the rearrangement of dislocations. The severe stress imposed by hot-extrusion generates high density dislocations in the grains. Subsequently, the movement and arrangement of dislocations form lots of small angle grain-boundaries, refining initial grains into several substructure. In addition to the refinement of grains, hot deformation promotes homogeneous precipitation of hardening particles in matrix, particularly Al₃Zr compound, which can pin the movement of dislocations to restrain grains coarsening during recrystallization effectively[17].

3.3 Microstructure and properties of alloy after heat treatment

The as-extruded alloy was subjected to 480 solid solution and 120 single-step aging. It can be seen from XRD spectrum shown in Fig.2 that the diffraction peaks of secondary phases have completely disappeared after solution, which suggests a good re-dissolution effect. Vickers hardness at different time was measured and plotted in Fig.5. It is apparent that the hardness increases rapidly at the initial stage. At about 14 h, the value reaches a peak of HV 156 and then

decreases slowly. After being aged for 44 h, another hardening peak appears with HV 153.

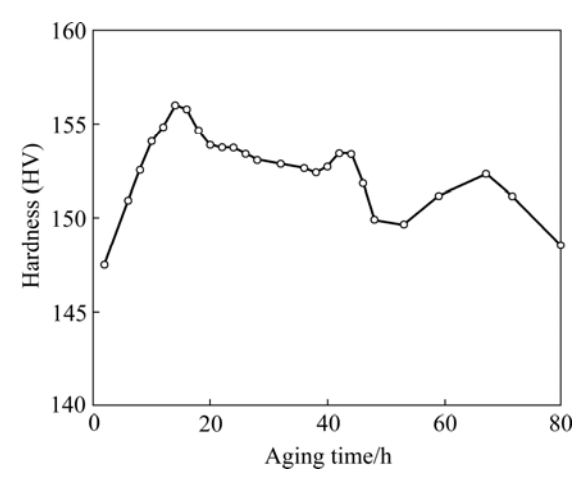


Fig.5 Relationship between hardness and aging time at 120 temper

In order to study the relationship between aging properties and microstructure, TEM was used to characterize the morphologies and precipitated particles in the aging alloy. Fig.6 shows the TEM bright field images and the SADE pattern of the specimen after being aged for 14 h. It can be seen that a large quantity of dark precipitates less than 5 nm in diameter are uniformly distributed in the matrix. The precipitates are identified as intermediate η' -phase (MgZn), as a series of additional

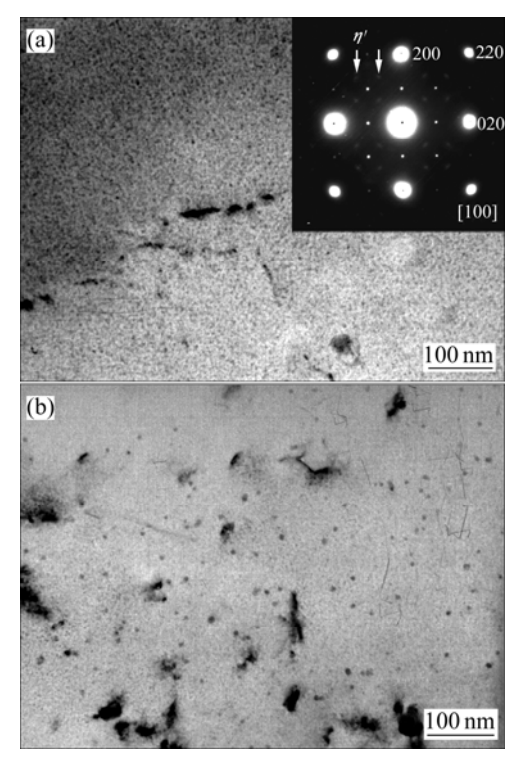


Fig.6 TEM micrographs and SAED pattern of SFed Al-11.5Zn-2.0Mg-1.6Cu alloy after being aged at 120 for 14 h: (a) η' precipitates; (b) Al₃Zr particles

diffraction spots appear at (2/3, 2/3, 0), (2/3, 4/3, 0), (4/3, 2/3, 0) and (4/3, 4/3, 0) positions in the Al[100] zone axis pattern[18–19]. It is noticeable that the superlattice spots in (110) positions are generated from Al₃Zr particles, which take spherical shape with an approximate average diameter of 10 nm. The TEM morphology and SAED pattern of another specimen which is aged for 44 h are shown in Fig.7. The coarsening of precipitates occurs with the increase of aging time. The diffraction spots at (2/3, 2/3, 0), (2/3, 4/3, 0), (4/3, 2/3, 0) and (4/3, 4/3, 0) positions get stronger compared with those in Fig.6, which suggests that the volume fraction of η' phase increases after being aged for 44 h.

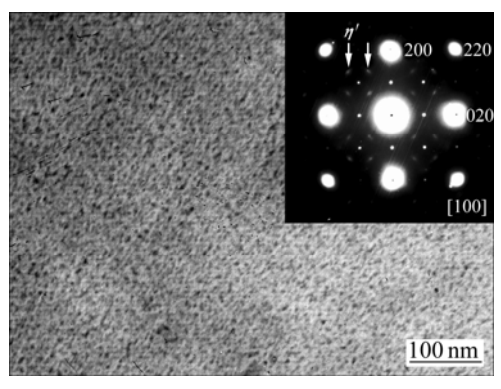


Fig.7 TEM micrograph and SAED pattern of SFed Al-11.5Zn-2.0Mg-1.6Cu alloy after being aged at 120 for 44 h

4 Conclusions

- 1) The microstructure consists of equiaxed and uniform grains with an average size of about 25 μm in the central region of the spray-formed Al-11.5Zn-2.0Mg-1.6Cu billet. Fine and irregular morphologies are present in the bottom and top regions. Both the grain boundary and intragranular phases are identified as intermetallics MgZn₂ dissolving considerable amount of Cu element.
- 2) Hot deformation process promotes the microstructural refinement. After hot extrusion, the large-size grain boundary and intragranular phase disappear, instead, η -phase(MgZn₂) and Al₃Zr phase particles precipitate in the matrix.
- 3) The maximum hardness is achieved after being aging at 120 for 14 h associated with a massive precipitation of intermediate η' phase in the matrix.

References

- [1] PLIES J B, GRANT N J. Structure and properties of spray formed 7150 containing Fe and Si[J]. The International Journal of Powder Metallurgy, 1994, 30(3): 335–343.
- [2] SANCTIS M D. Structure and properties of rapidly solidified ultrahigh strength Al-Zn-Mg-Cu alloys produced by spray deposition[J]. Materials Science and Engineering A, 1991, 141: 103.
- [3] SHARMA M M, AMATEAU M F, EDEN T J. Hardening

- mechanisms of spray formed Al-Zn-Mg-Cu alloys with scandium and other elemental additions[J]. Journal of Alloys and Compounds, 2006, 416: 135–142
- [4] WANG Feng, XIONG Bai-qing, ZHANG Yong-an, ZHU Bao-hong, LIU Hong-wei, WANG Zi-xing, HE Xiao-qing. Microstructure and mechanical properties of spray-deposited Al-10.8Zn-2.8Mg-1.9Cu alloy after two-step aging treatment at 110 and 150 [J]. Materials Characterization, 2007, 58(1): 82–86.
- [5] MÄCHLER R, UGGOWITZER P J, SOLENTHALER C, PEDRAZZOLI R M, SPEIDEL M O. Structure, mechanical properties, and stress corrosion behaviour of high strength spray deposited 7000 series aluminium alloy[J]. Materials and Science and Technology, 1991, 7(5): 447–451.
- [6] GRANT P S. Spray forming[J]. Progress in Materials Science, 1995, 39(4/5): 497–545.
- [7] KANG Fu-wei, ZHANG Guo-qing, LI Zhou, SUN Jian-fei. Hot deforming of spray forming nickel-base superalloy using processing maps[J]. Trans Nonferrous Met Soc China, 2008, 18(3): 531–535.
- [8] RAJU K, OJHA S N, HARSHA A P. Spray forming of aluminum alloys and its composites: an overview[J]. Journal of Materials Science, 2008, 43(8): 2509–2521.
- [9] XU Q, LAVERNIA E J. Microstructural evolution during the initial stages of spray atomization and deposition[J]. Scripta Materialia, 1999, 41(5): 535–540.
- [10] GRANT P S. Solidification in spray forming[J]. Metallurgical and Materials Transactions A: Physical Metallurgy and Materials Science, 2007, 38A(7): 1520–1529.
- [11] MONDOLFO L F. Aluminium alloys: Structure and properties[M]. London: Butterworths Publication, 1976: 577–584.
- [12] MONDAL C, MUKHOPADHYAY A K. On the nature of

- $T(Al_2Mg_3Zn_3)$ and $S(Al_2CuMg)$ phases present in as-cast and annealed 7055 aluminum alloy[J]. Materials Science and Engineering A, 2005, 391(1/2): 367–376.
- [13] WANG F, XIONG B Q, ZHANG Y A, ZHANG Z H, WANG Z X, ZHU B H, LIU H. Microstructure and mechanical properties of spray-deposited Al-Zn-Mg-Cu alloy[J]. Materials and Design, 2007, 28(10): 1154–1158.
- [14] XU C, FURUKAWA M, HORITA Z, LANGDON T G. Influence of ECAP on precipitate distributions in a spray-cast aluminum alloy[J]. Acta Materialia, 2005, 53(3): 749-758.
- [15] DESCHAMPS A, BRECHET Y. Influence of quench and heating rates on the ageing response of an Al-Zn-Mg-(Zr) alloy[J]. Materials Science and Engineering A, 1998, 251(1/2): 200–201.
- [16] WEI Qiang, XIONG Bai-qing, ZHANG Yong-an, ZHU Bao-hong, SHI Li-kai. Production of high strength Al-Zn-Mg-Cu alloys by spray forming process[J]. Trans Nonferrous Met Soc China, 2001, 11(2): 258–261.
- [17] NAM C Y, HAN J H, CHUNG Y H, SHIN M C. Effect of precipitates on microstructural evolution of 7050 Al alloy sheet during equal channel angular rolling[J]. Materials Science and Engineering A, 2003, 347(1/2): 253–257.
- [18] FAN X G, JIANG D M, MENG Q C, LAI Z H, ZHANG X M. Characterization of precipitation microstructure and properties of 7150 aluminium alloy[J]. Materials Science and Engineering A, 2006, 427(1/2): 130–135.
- [19] GANG SHA, ALFRED CEREZO. Early-stage precipitation in Al-Zn-Mg-Cu alloy (7050)[J]. Acta Materialia, 2004, 52(15): 4503-4516.

(Edited by CHEN Can-hua)